This article was downloaded by: [Renmin University of China]
On: 13 October 2013, At: 10:51
Publisher: Taylor & Francis
Informa Ltd Registered in England and Wales Registered Number: 1072954 Registered office: Mortimer House, 37-41 Mortimer Street, London W1T 3JH, UK

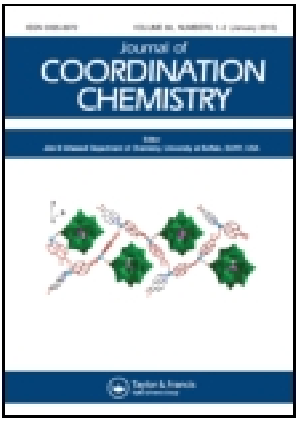

Journal of Coordination Chemistry
Publication details, including instructions for authors and subscription information:
http://www.tandfonline.com/loi/gcoo20

Syntheses, crystal structures, and fluorescent properties of two 2-D Cd(II) complexes based on 2-((1H-1,2,4-triazol-1-yl)methyl)-1H-benzimidazole and 1,2,4,5-benzenetetracarboxylate

Xiao Han [a] , Xiuxiu Wang [a] , Guanghua Jin [a] & Xiangru Meng [a]
[a] The College of Chemistry and Molecular Engineering , Zhengzhou University , Zhengzhou , P.R. China

Accepted author version posted online: 24 Jan 2013.Published online: 15 Mar 2013.

To cite this article: Xiao Han , Xiuxiu Wang , Guanghua Jin & Xiangru Meng (2013) Syntheses, crystal structures, and fluorescent properties of two 2-D Cd(II) complexes based on 2-((1H-1,2,4-triazol-1-yl)methyl)-1H-benzimidazole and 1,2,4,5-benzenetetracarboxylate, Journal of Coordination Chemistry, 66:5, 800-812, DOI: 10.1080/00958972.2013.769210

To link to this article: http://dx.doi.org/10.1080/00958972.2013.769210

PLEASE SCROLL DOWN FOR ARTICLE

Taylor & Francis makes every effort to ensure the accuracy of all the information (the "Content") contained in the publications on our platform. However, Taylor & Francis, our agents, and our licensors make no representations or warranties whatsoever as to the accuracy, completeness, or suitability for any purpose of the Content. Any opinions and views expressed in this publication are the opinions and views of the authors, and are not the views of or endorsed by Taylor & Francis. The accuracy of the Content should not be relied upon and should be independently verified with primary sources of information. Taylor and Francis shall not be liable for any losses, actions, claims, proceedings, demands, costs, expenses, damages, and other liabilities whatsoever or howsoever caused arising directly or indirectly in connection with, in relation to or arising out of the use of the Content.

This article may be used for research, teaching, and private study purposes. Any substantial or systematic reproduction, redistribution, reselling, loan, sub-licensing, systematic supply, or distribution in any form to anyone is expressly forbidden. Terms &

Journal of Coordination Chemistry
Vol. 66, No. 5, 10 March 2013, 800–812

Syntheses, crystal structures, and fluorescent properties of two 2-D Cd(II) complexes based on 2-((1*H*-1,2,4-triazol-1-yl) methyl)-1*H*-benzimidazole and 1,2,4,5-benzenetetracarboxylate

XIAO HAN, XIUXIU WANG, GUANGHUA JIN and XIANGRU MENG*

The College of Chemistry and Molecular Engineering, Zhengzhou University, Zhengzhou, P.R. China

(*Received 21 May 2012; in final form 4 October 2012*)

Two complexes formulated as $\{[Cd(btec)_{0.5}(tmb)H_2O]\cdot 4H_2O\}_n$ (**1**) and $\{[Cd(H_2btec)(tmb)(H_2O)]\cdot 2H_2O\}_n$ (**2**) ($H_4btec = 1,2,4,5$-benzenetetracarboxylic acid, tmb = 2-((1*H*-1,2,4-triazol-1-yl) methyl)-1*H*-benzimidazole) have been synthesized and characterized by elemental analysis, IR, and single crystal X-ray diffraction. Single crystal X-ray diffraction shows that **1** has a 2-D layer structure in which tmb bridges and all of the carboxylates from 1,2,4,5-benzenetetracarboxylate chelate. In **2** Cd(II) ions are bridged by monodentate carboxylates leading to a 2-D layer structure with all tmb ligands coordinated monodentate to Cd(II), hanging at two sides of the layers. Complexes **1** and **2** are further extended to 3-D supramolecular structures by hydrogen bonding interactions. Luminescent properties have been investigated in the solid state at room temperature.

Keywords: 2-((1*H*-1,2,4-Triazol-1-yl)methyl)-1*H*-benzimidazole; Cadmium complex; Crystal structure

1. Introduction

Design and construction of complexes with specific structures continues to be a productive research area with fascinating structural diversities and potential applications [1–3]. A variety of complexes have been prepared under hydrothermal conditions by using *N*-heterocyclic ligands and aromatic polycarboxylates, like triazole, benzotriazole, tetrazole, and their derivatives, and 1,2-benzenedicarboxylate, 1,3-benzenedicarboxylate, 1,4-benzenedicarboxylate, 1,3,5-benzenetricarboxylate, 1,2,4-benzenetricarboxylate, and 1,2,4,5-benzenetetracarboxylate [4–9]. But control in constructing complexes with desired structures and physical properties still remains a major challenge. Thus, work is required to extend knowledge of relevant structural types and establish proper synthetic strategies for desirable complexes.

Metal and coordinating possibilities, metal-to-ligand ratio, the flexibility of the organic building blocks, the number and orientation of the coordination sites in organic spacers, functionality and denticity of ligands, the solvent system, the pH of the solution, and selection of anions influence the formation of complexes [10–12]. Selection of anions

---

*Corresponding author. Email: mxr@zzu.edu.cn

Journal of Coordination Chemistry
ISSN 0095-8972 print/ISSN 1029-0389 online
http://dx.doi.org/10.1080/00958972.2013.769210

plays conclusive roles in the construction and structural tuning of resulting complexes. In order to control structures of complexes, the geometry and size of the corresponding anions can be changed, even for complexes containing neutral ligands [13–16]. Thus, study of the influence of anions on the final structures of complexes has attracted considerable attention [17,18].

Herein, we select 2-((1*H*-1,2,4-triazol-1-yl)methyl)-1*H*-benzimidazole (tmb) which has abundant *N*-donor sites and 1,2,4,5-benzenetetracarboxylic acid (H_4btec) which may be partially or completely deprotonated as ligands. Through reactions of CdI_2 or $Cd(Ac)_2{\cdot}2H_2O$ with tmb and H_4btec, two new 2-D complexes, $\{[Cd(btec)_{0.5}(tmb)H_2O]{\cdot}4H_2O\}_n$ (**1**) and $\{[Cd(H_2btec)(tmb)(H_2O)]{\cdot}2H_2O\}_n$ (**2**), were obtained. Elemental analyses, IR, single-crystal X-ray diffraction, and fluorescent properties have been determined.

2. Experimental

2.1. *General information and materials*

2-((1*H*-1,2,4-triazol-1-yl)methyl)-1*H*-benzimidazole was synthesized according to the literature [19]. All reagents and solvents employed were of AR Grade from commercial sources and used as received. IR data were recorded on a BRUKER TENSOR 27 spectrophotometer with KBr pellets from 400 to 4000 cm^{-1}. Elemental analyses (C, H, and N) were carried out on a FLASH EA 1112 elemental analyzer. Solid-state luminescence spectra were recorded with a Fluoro Max-P fluorescence spectrophotometer. Powder X-ray diffraction (PXRD) patterns were recorded using Cu Kα radiation on a PANalytical X'Pert PRO diffractometer.

2.2. *Synthesis of* $\{[Cd(btec)_{0.5}(tmb)H_2O]{\cdot}4H_2O\}_n$ *(1)*

A mixture of 2-((1*H*-1,2,4-triazol-1-yl)methyl)-1*H*-benzimidazole (0.05 mM), CdI_2 (0.05 mM), 1,2,4,5-benzenetetracarboxylic acid (0.05 mM), H_2O (4 mL), and CH_3OH (4 mL) was poured into a Teflon-lined stainless steel vessel (25 mL), then the vessel was sealed and heated to 120 °C for 3 days. The autoclave was cooled to room temperature at 10 °C h^{-1}. Crystals of $\{[Cd(btec)_{0.5}(tmb)H_2O]{\cdot}4H_2O\}_n$ suitable for X-ray analysis were collected. Anal. Calcd for $C_{15}H_{20}CdN_5O_9$ (%): C, 34.20; H, 3.83; N, 13.30. Found (%): C, 33.78; H, 3.98; N, 13.04. IR (KBr, cm^{-1}): 3448 (m), 3099 (m), 2930 (m), 1649 (s), 1540 (w), 1519 (m), 1491 (w), 1450 (m), 1386 (s), 1344 (m), 1313 (w), 1278 (m), 1132 (s), 902 (w), 877 (w), 846 (w), 780 (w), 759 (w), 744 (s).

2.3. *Synthesis of* $\{[Cd(H_2btec)(tmb)(H_2O)]{\cdot}2H_2O\}_n$ *(2)*

The synthesis of **2** was similar to that described for **1** except using $Cd(Ac)_2{\cdot}2H_2O$ instead of CdI_2. Crystals of $\{[Cd(H_2btec)(tmb)(H_2O)]{\cdot}2H_2O\}_n$ suitable for X-ray analysis were obtained. Anal. Calcd for $C_{20}H_{19}CdN_5O_{11}$ (%): C, 38.88; H, 3.10; N, 11.34. Found (%): C, 37.67; H, 2.93; N, 11.92. IR (KBr, cm^{-1}): 3404 (m), 3105 (m), 1624 (m), 1558 (s), 1497 (m), 1440 (m), 1387 (s), 1327 (m), 1285 (m), 1137 (m), 913 (w), 844 (w), 834 (s), 817 (w), 773 (w), 741 (s).

Table 1. Crystal data and structure refinement data of **1** and **2**.

Complex	**1**	**2**
Empirical formula	$C_{15}H_{20}CdN_5O_9$	$C_{20}H_{19}CdN_5O_{11}$
Formula weight	526.76	617.80
Temperature (K)	293(2)	293(2)
Crystal system	Triclinic	Triclinic
Space group	$P\bar{1}$	$P\bar{1}$
Unit cell dimensions (Å, °)		
a	9.916(2)	7.8291(16)
b	10.291(2)	9.793(2)
c	10.700(2)	15.930(3)
α	111.07(3)	105.41(3)
β	101.56(3)	103.10(3)
γ	97.93(3)	96.36(3)
Volume (Å^3)	971.5(3)	1127.6(4)
Z	2	2
Calculated density (Mg m^{-3})	1.801	1.820
Absorption coefficient (mm^{-1})	1.185	1.042
F(000)	530	620
θ range for data collection, deg	2.12–27.92	2.19–27.88
h range	$-13 \leqslant h \leqslant 13$	$-10 \leqslant h \leqslant 10$
k range	$-13 \leqslant k \leqslant 13$	$-12 \leqslant k \leqslant 12$
l range	$-14 \leqslant l \leqslant 14$	$-20 \leqslant l \leqslant 20$
Crystal sizes (mm^3)	0.19 × 0.16 × 0.15	0.19 × 0.17 × 0.11
R(int)	0.0201	0.0262
Data/restraints/parameters	4585/0/271	5351/0/336
Goodness-of-fit on F^2	1.022	1.048
Final R indices [$I > 2\sigma(I)$]	$R_1 = 0.0247 wR_2 = 0.0565$	$R_1 = 0.0278 wR_2 = 0.0645$
R indices (all data)	$R_1 = 0.0270 wR_2 = 0.0580$	$R_1 = 0.0307 wR_2 = 0.0666$
$\Delta\rho_{\text{fin}}$ (max/min), e Å^{-3}	0.571 and −0.512	0.673 and −0.621

Table 2. Selected bond lengths (Å) and angles (°) for **1** and **2**.

*Complex **1***					
Cd(1)–O(1)	2.4500(17)	Cd(1)–O(2)	2.3902(19)	Cd(1)–O(3)#2	2.3879(17)
Cd(1)–O(4)#2	2.4873(16)	Cd(1)–O(5)	2.4454(18)	Cd(1)–N(1)	2.3198(19)
Cd(1)–N(5)#1	2.293(2)	O(1)–Cd(1)–O(4)#2	148.08(6)	O(5)–Cd(1)–O(4)#2	72.96(6)
N(5)#1–Cd(1)–O(3)#2	136.97(6)	N(5)#1–Cd(1)–N(1)	89.87(7)	N(5)#1–Cd(1)–O(2)	137.65(6)
N(1)–Cd(1)–O(2)	96.47(7)	O(3)#2–Cd(1)–O(2)	83.98(6)	N(1)–Cd(1)–O(3)#2	96.38(6)
N(1)–Cd(1)–O(5)	175.69(6)	N(5)#1–Cd(1)–O(5)	89.24(7)	O(2)–Cd(1)–O(5)	87.02(6)
N(5)#1–Cd(1)–O(1)	84.35(7)	N(1)–Cd(1)–O(1)	106.67(7)	O(3)#2–Cd(1)–O(5)	81.43(6)
O(2)–Cd(1)–O(1)	53.69(6)	O(3)#2–Cd(1)–O(1)	133.03(6)	N(5)#1–Cd(1)–O(4)#2	83.58(7)
O(5)–Cd(1)–O(1)	77.44(7)	O(3)#2–Cd(1)–O(4)#2	53.49(6)	N(1)–Cd(1)–O(4)#2	102.74(7)
O(2)–Cd(1)–O(4)#2	134.58(6)				
*Complex **2***					
Cd(1)–O(1)	2.2289(17)	Cd(1)–O(5)	2.2611(19)	Cd(1)–O(8)#1	2.2753(17)
Cd(1)–O(9)	2.2783(17)	Cd(1)–N(1)	2.302(2)	O(9)–Cd(1)–N(1)	83.15(7)
O(1)–Cd(1)–O(5)	116.56(7)	O(1)–Cd(1)–O(8)#1	88.56(7)	O(1)–Cd(1)–O(9)	124.36(7)
O(5)–Cd(1)–O(8)#1	83.26(6)	O(5)–Cd(1)–O(9)	117.90(6)	O(8)#1–Cd(1)–O(9)	87.15(6)
O(1)–Cd(1)–N(1)	104.08(8)	O(5)–Cd(1)–N(1)	93.60(7)	O(8)#1–Cd(1)–N(1)	166.97(7)

Symmetry transformations used to generate equivalent atoms: For **1**: #1: $-x+1$, $-y+1$, $-z$; #2 $-x+1$, $-y+2$, $-z+1$. For **2**: #1: $x-1$, y, z.

2.4. *Single-crystal structure determination*

A suitable single crystal of **1** or **2** was carefully selected and glued to a thin glass fiber. Crystal structure determination by X-ray diffraction was performed on a Rigaku Saturn 724 CCD area detector with a graphite monochromator for the X-ray source (Mo–Kα radiation,

Table 3. Hydrogen bonds of **1** and **2**.

D–H···A	*d*(D–H) (Å)	*d*(H···A) (Å)	*d*(D···A) (Å)	(D–H···A) (°)
*Complex **1***				
O(6)–H(6B)···O(8)	0.84	1.90	2.738(3)	176.3
O(7)–H(7B)···O(8)	0.84	2.00	2.773(4)	151.6
O(8)–H(8A)···O(5)	0.85	2.40	2.964(3)	124.1
O(8)–H(8B)···O(9)#4	0.85	2.28	2.934(4)	133.5
N(2)–H(2)···O(6)#1	0.86	2.02	2.822(3)	154.4
O(5)–H(5B)···O(2)#2	0.85	1.91	2.756(3)	171.1
O(5)–H(5A)···O(6)#4	0.85	2.16	2.890(3)	144.0
O(6)–H(6A)···O(3)#4	0.84	1.97	2.739(3)	151.3
O(7)–H(7A)···O(1)#4	0.85	1.95	2.757(3)	159.8
O(9)–H(9A)···O(4)#5	0.85	1.91	2.761(3)	179.6
O(9)–H(9B)···O(7)#6	0.85	1.90	2.747(3)	179.7
*Complex **2***				
N(5)–H(5A)···O(10)	0.86	1.81	2.610(3)	152.9
O(6)–H(6)···O(3)#2	0.82	1.97	2.619(2)	135.0
O(2)–H(2)···N(4)#1	0.82	1.92	2.656(3)	148.9
O(9)–H(9B)···O(7)#1	0.85	1.80	2.599(2)	154.4
O(10)–H(10B)···O(11)#1	0.85	2.27	3.081(4)	159.9
O(9)–H(9A)···O(5)#5	0.84	1.92	2.748(2)	168.0
O(10)–H(10A)···O(1)#6	0.85	2.00	2.755(3)	147.8
O(11)–H(11B)···O(8)#6	0.85	2.15	2.910(3)	148.1
O(11)–H(11A)···O(3)#7	0.85	2.19	3.032(3)	170.0

Symmetry transformations used to generate equivalent atoms: For **1**: #1: $-x+1, -y+1, -z$; #2: $-x+1, -y+2, -z+1$; #4: $-x+1, -y+1, -z+1$; #5: $x, y-1, z$; #6: $x+1, y, z$. For **2**: #1: $x-1, y, z$; #2: $x+1, y, z$; #5: $-x, -y+2, -z+1$; #6: $x, y-1, z$; #7: $x+1, y-1$, z.

$\lambda = 0.71073$ Å) operating at 50 kV and 40 mA. The data were collected by ω scan mode at 293(2) K; the crystal-to-detector distance was 45 mm. An empirical absorption correction was applied and the data were corrected for Lorentz and polarization effects. The structures were solved by direct methods and refined by full-matrix least-squares and difference Fourier techniques, based on F^2, using SHELXS-97 [20]. All nonhydrogen atoms were refined anisotropically. Hydrogens were positioned geometrically and refined using a riding model. All hydrogens were included in the final refinement. Crystallographic parameters and structural refinement for the complexes are summarized in table 1. Selected bond lengths and angles of the complexes are listed in table 2. Hydrogen bonds are listed in table 3.

3. Results and discussion

3.1. *IR spectroscopy of 1 and 2*

IR spectra show absorptions at 3448 cm^{-1} for **1** and 3404 cm^{-1} for **2** attributed to the O–H stretch. Absorptions at 3099 cm^{-1} for **1** and 3105 cm^{-1} for **2** originate from Ar–H stretching vibrations. Four sharp absorptions at 1649, 1519, 1491, and 1450 cm^{-1} for **1** and 1624, 1558, 1497, and 1440 cm^{-1} for **2** are due to C=C and C=N stretches. Absorptions at 744 cm^{-1} for **1** and 741 cm^{-1} for **2** correspond to characteristic stretching vibrations of 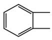. Absorptions at 780 and 759 cm^{-1} for **1** and 844 and 773 cm^{-1} for **2** belong to stretching vibrations of 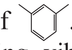. Absorptions at 846 cm^{-1} for **1** and 834 cm^{-1} for **2** can be attributed to the stretching vibrations of 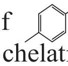. Separations (Δ) between υ_a(COO) and υ_s(COO) are different for unidentate and chelating carboxylates [21,22]. In **1**, carboxylates have υ_a(COO) and υ_s(COO) at 1540 and 1491 cm^{-1} ($\Delta = 49\ \mathrm{cm}^{-1}$). This Δ value is comparable to those of chelating carboxylates. Different from **1**, carboxylates in **2** coordinate unidentate to Cd(II), and Δ between υ_a(COO) and υ_s(COO) is 171 cm^{-1} (1558 and 1387 cm^{-1}). The above analyses are consistent with results of X-ray diffraction.

3.2. *Crystal structures of $\{[Cd(btec)_{0.5}(tmb)H_2O]\cdot 4H_2O\}_n$ (1)*

The X-ray crystallographic analysis reveals that **1** crystallizes in the triclinic space group $P\bar{1}$. Cd(II) exhibits a slightly distorted pentagonal bipyramidal geometry formed by five oxygens (Cd1-O1 = 2.4500(17) Å, Cd1-O2 = 2.3902(19) Å, Cd1-O3$^{\#2}$ = 2.3879(17) Å, Cd1-O4$^{\#2}$ = 2.4873(16) Å, and Cd1-O5 = 2.4454(18) Å) from two 1,2,4,5-benzenetetracarboxylate groups and one water and two nitrogens (Cd1-N1 = 2.3198(19) Å, Cd1-N5$^{\#1}$ = 2.293(2) Å) of two tmb ligands (figure 1(a)). These Cd–O and Cd–N bond lengths are close to those in the related [Cd(BDC)(phen)·DMF] (H_2BDC=benzene-1,4-dicarboxylic acid, phen=1,10-phenanthroline) [23], $[Cd(tmb)_2(Cl)_2(H_2O)_2]\cdot 4H_2O$ [24]. O1, O2, O3$^{\#2}$, O4$^{\#2}$, N5$^{\#1}$, and Cd1 form an equatorial plane (the mean deviation from plane is 0.4395 Å), while O5 and N1 occupy axial positions. The N1–Cd1–O5 bond angle is 175.69(6)°. As shown in figure 1(b), each 1,2,4,5-benzenetetracarboxylate links four Cd(II) ions to form an infinite 1-D chain parallel to the *a* direction and all carboxylates chelate (scheme 1, mode I). The Cd···Cd distance separated by meta-carboxylates (9.916 Å) is longer than the Cd···Cd distance separated by ortho-carboxylates (5.386 Å) but slightly shorter than the distance separated by para-carboxylates (11.350 Å). The 1-D chains are further interlinked through two bridging tmb to form a 2-D layer along the *ab* plane and Cd···Cd distance separated by bridging tmb is 7.140 Å. There are ten O–H···O hydrogen bonds and one N–H···O hydrogen bond (table 3). The layers are further connected by the 11 hydrogen bonds to generate a 3-D supramolecular framework (figure 1(c)).

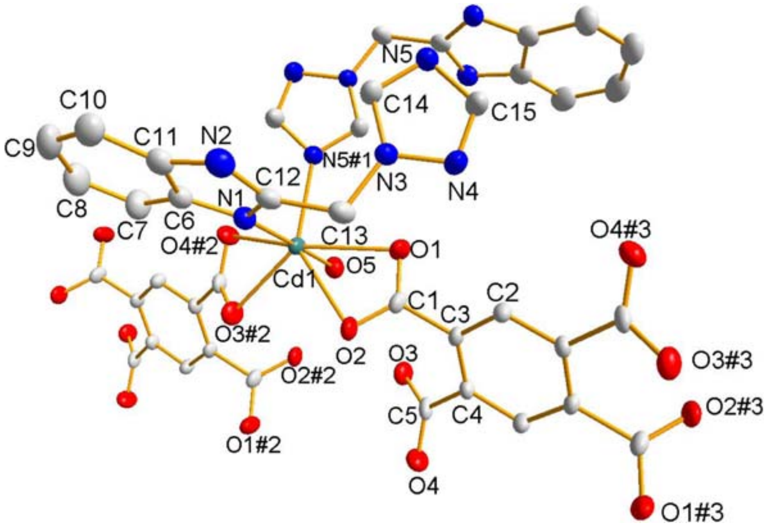

Figure 1a. Coordination environment of Cd(II) in **1** with atom numbering scheme; hydrogens and free waters were omitted for clarity.

3.3. Crystal structure of $\{[Cd(H_2btec)(tmb)(H_2O)]\cdot 2H_2O\}_n$ (2)

Since coordination modes of ligands can be influenced by anions [15, 16], we introduced CH_3COO^-, and obtained **2**, with a different structure than **1**. In **2**, tmb are monodentate (scheme 2, mode I) and carboxylates of 1,2,4,5-benzenetetracarboxylate groups coordinate monodentate to Cd(II) (scheme 1, modes II and III), but in **1**, tmb was bridging (scheme 2, mode II) and all carboxylates of 1,2,4,5-benzenetetracarboxylate chelate (scheme 1, mode I). As depicted in figure 2(a), the central Cd(II) is five coordinate in a distorted trigonal bipyramidal geometry with four oxygens and one nitrogen. Three oxygens from two carboxylates and one water occupy the equatorial positions (the mean deviation from plane is 0.0532 Å), and one nitrogen from triazole with one oxygen from carboxylate locate in apical positions (the O8$^{\#1}$–Cd1–N1 bond angle is 166.97(7)°). The Cd–O bond lengths (Cd1-O1 = 2.2289(17) Å; Cd1-O5 = 2.2611(19) Å; Cd1–O8$^{\#1}$ = 2.2753(17) Å, and Cd1–O9 = 2.2783(17) Å) in **2** are slightly shorter than those in **1** but are close to those in the related $[Cd_2(btec)(phen)_2(H_2O)_2]$ [23]. The Cd–N bond lengths (Cd1–N1 = 2.302(2) Å) are

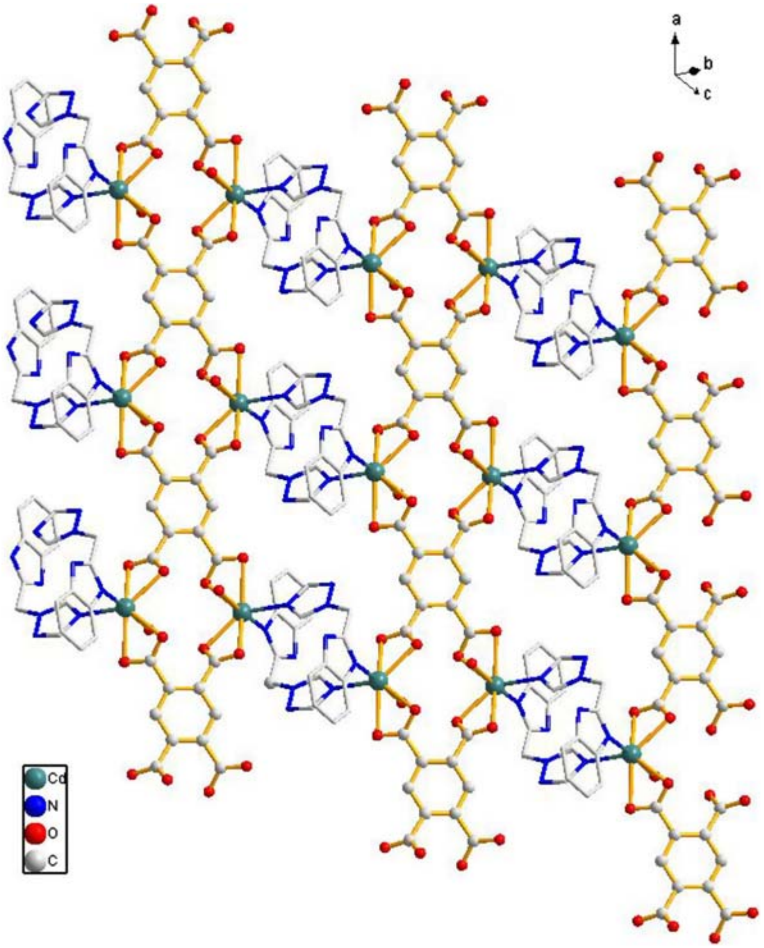

Figure 1b. View of the 2-D plane structure of **1**.

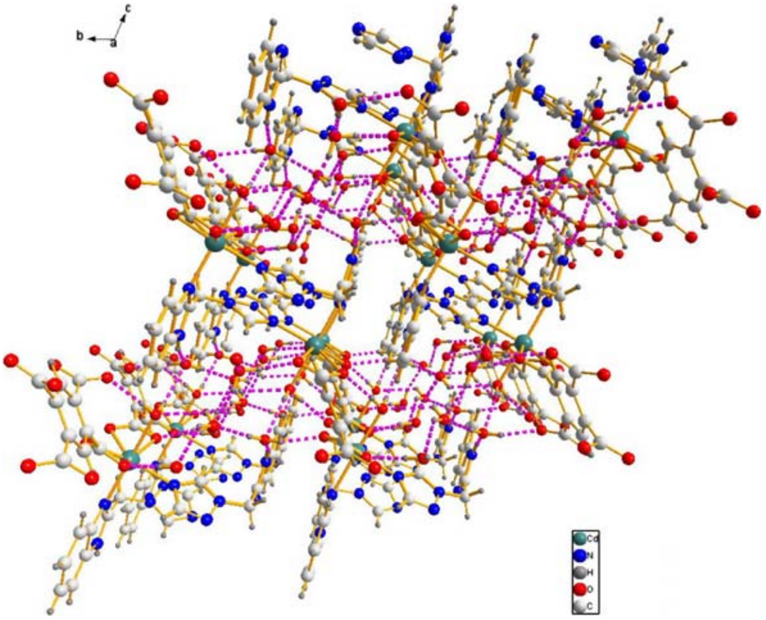

Figure 1c. View of the crystal packing of **1**; the 3-D structure is formed by hydrogen bonds.

close to those in **1** and [Cd_2(btec)$(phen)_2$$(H_2O)_2$]. There are two crystallographically independent 1,2,4,5-benzenetetracarboxylates (figure 2(b)) in **2** (scheme 1, modes II and III). One 1,2,4,5-benzenetetracarboxylate coordinates monodentate to four Cd(II) ions forming

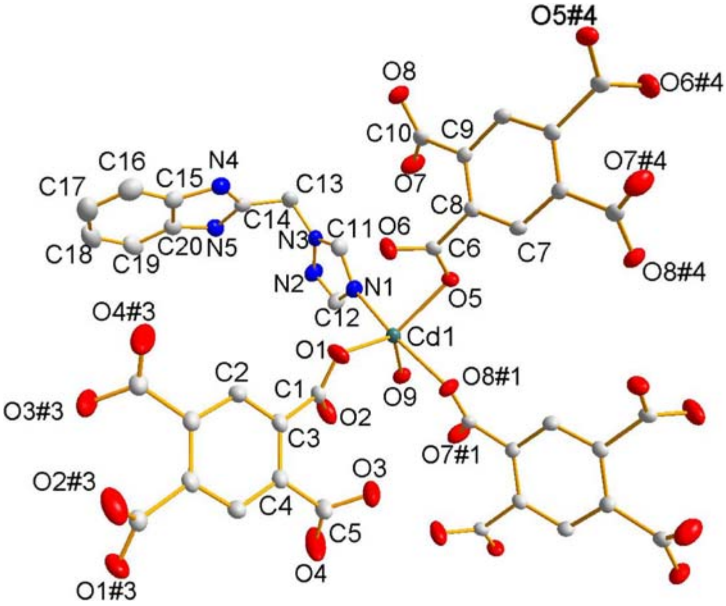

Figure 2a. Coordination environment of Cd(II) in **2** with atom numbering scheme; hydrogens and free waters were omitted for clarity.

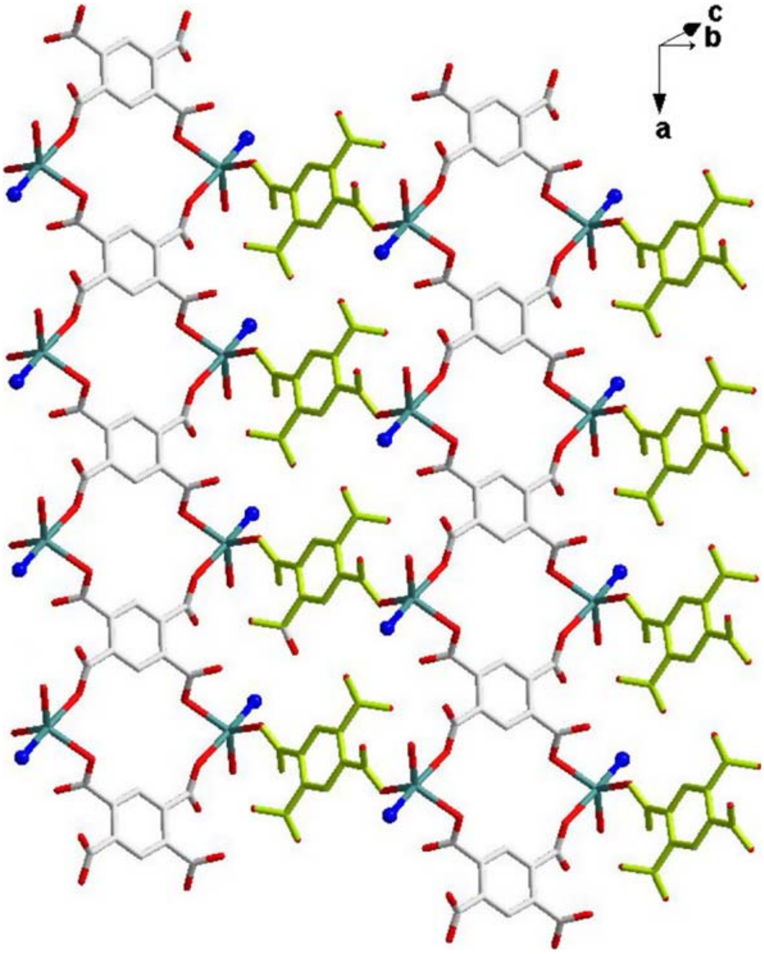

Figure 2b. View of the 2-D corrugated plane structure of **2**. Part of the tmb ligands are omitted for clarity.

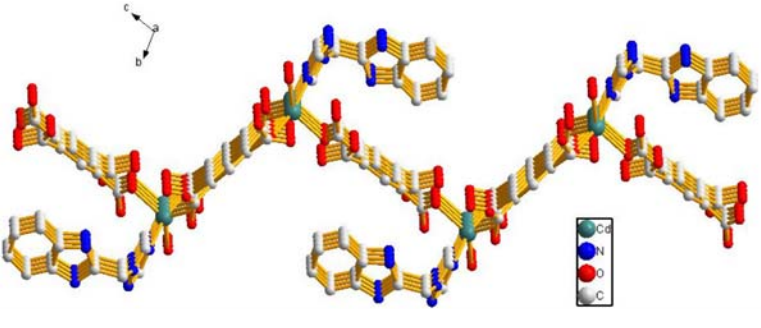

Figure 2c. 2-D structure of **2** showing tmb ligands hanging at two sides of the layer.

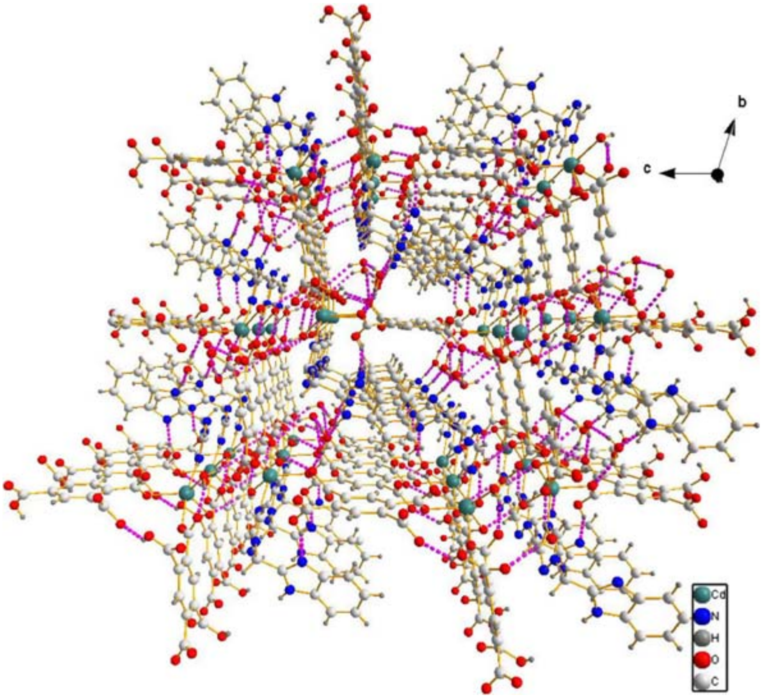

Figure 2d. View of the crystal packing of **2**; the 3-D structure is formed by hydrogen bonds.

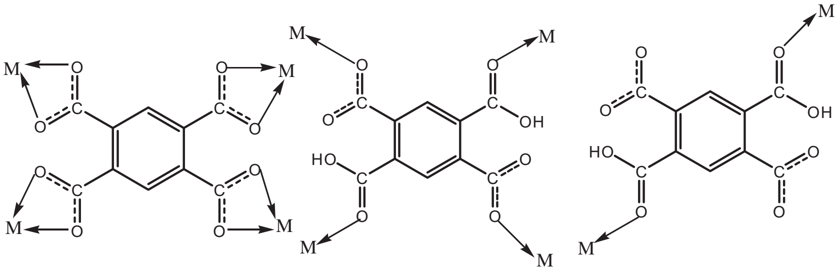

mode I

mode II

mode III

Scheme 1. Coordination modes of 1,2,4,5-benzenetetracarboxylate found in complexes 1 and 2.

an infinite 1-D chain parallel to the *a* direction, while the other 1,2,4,5-benzenetetracarboxylate coordinates to two Cd(II) ions with monodentate para-carboxylates linking adjacent chains, further forming an undulating layer. All tmb ligands hang at two sides of the layer and the benzotriazole rings on the same side are parallel with distance between the neighboring benzotriazole rings of 6.8790 Å (figure 2c). There are seven O–H···O hydrogen bonds, one N–H···O hydrogen bond, and one O–H···N hydrogen bond (table 3). The corrugated layers transformed into a 3-D structure through the nine kinds of hydrogen bonds (figure 2d).

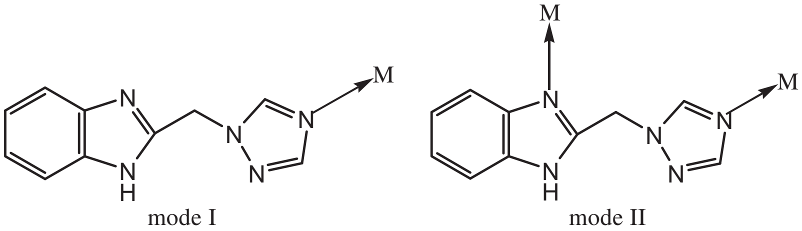

Scheme 2. Coordination modes of tmb found in complexes 1 and 2.

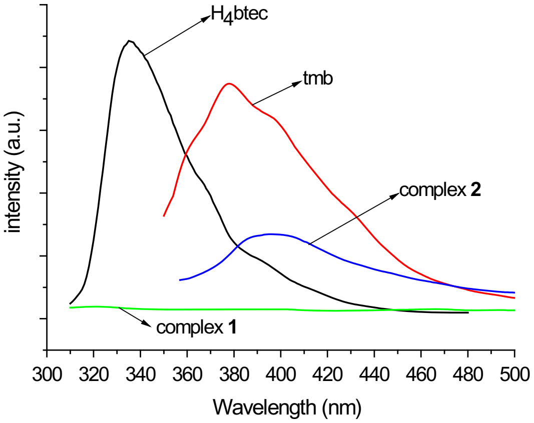

Figure 3. Solid-state emission spectra of H_4btec, tmb, **1** and **2** at room temperature.

3.4. *Luminescent properties*

A number of d^{10} transition metal complexes exhibit luminescence properties [25–27]. The solid-state fluorescence spectrum of H_4btec, tmb, **1** and **2** are depicted in figure 3. H_4btec exhibits an emission maximum at 335 nm upon excitation at 290 nm. The tmb displays an emission with a maximum at 378 nm upon excitation at 335 nm. The main emission for **2** was at 396 nm ($\lambda_{ex} = 353$ nm) and no clear photoluminescence was observed for **1**. The photoluminescence intensity of **1** and **2** is weaker than free tmb and H_4btec, attributed to competitive quenching effect of water [28]. Compared to the emission bands of the free ligands H_4btec and tmb, the emission spectrum of **2** shifts. The emission peak for **2** probably originates from the intraligand $\pi \rightarrow \pi^*$ transitions of tmb [29, 30]. The fluorescence intensity of **2** is stronger than that of **1** due to the different coordination environments of Cd(II) and the number of waters in the complexes.

3.5. *XRD patterns*

To confirm the phase purity of the complexes, the PXRD patterns were recorded for **1** and **2**, and the patterns were comparable to the corresponding simulated ones calculated from the single-crystal diffraction data (figures 4(a) and (b)), indicating a pure phase of each bulk sample.

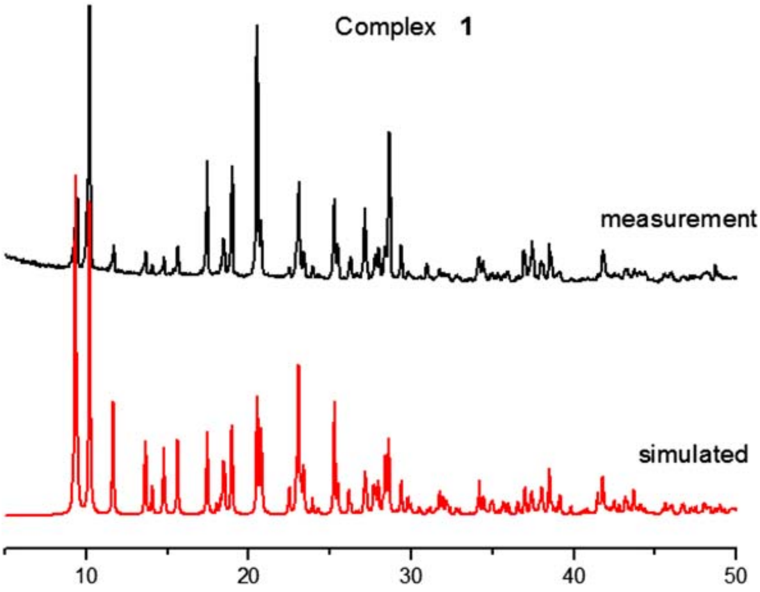

Figure 4a. The PXRD patterns of **1** at room temperature; simulated patterns are generated from single-crystal diffraction data.

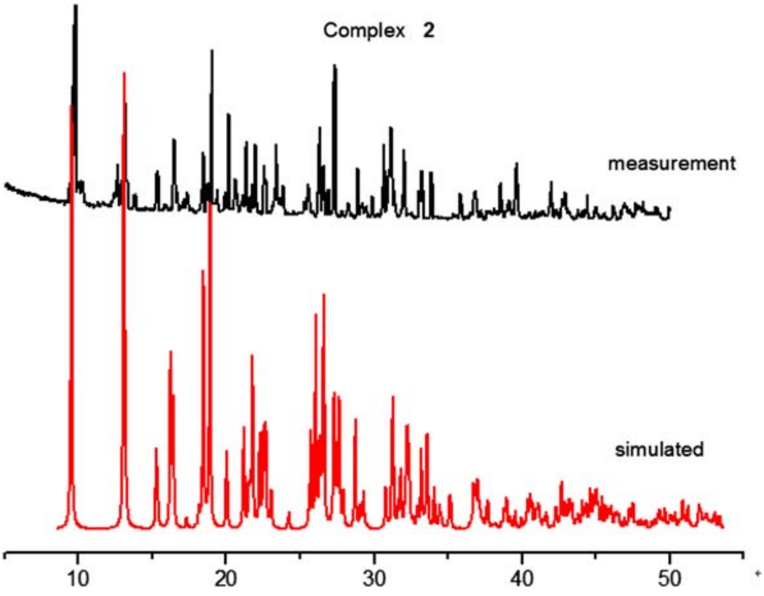

Figure 4b. The PXRD patterns of **2** at room temperature; simulated patterns are generated from single-crystal diffraction data.

4. Conclusion

Carboxylate and *N*-heterocyclic ligands play important roles in construction of complexes [31–33]. Through reactions of 2-((1*H*-1,2,4-triazol-1-yl)methyl)-1*H*-benzimidazole (tmb) with CdI_2 or $Cd(Ac)_2{\cdot}2H_2O$ in the presence of H_4btec, we obtained two new 2-D complexes $\{[Cd(btec)_{0.5}(tmb)H_2O]{\cdot}4H_2O\}_n$ (**1**) and $\{[Cd(H_2btec)(tmb)(H_2O)]{\cdot}2H_2O\}_n$ (**2**). In **1** and **2**, coordination environment of Cd(II) and coordination modes of tmb and 1,2,4,5-benzenetetracarboxylate are different. These results suggest that change of anions influences the coordination modes of carboxylate and *N*-heterocyclic ligand, influencing the coordination environment of the central metal ions and the detailed architecture of the complexes [13–16]. Similar behavior is observed in other complexes based on carboxylates and *N*-heterocyclic ligands [34–36]. Further efforts on the design and preparation of complexes with other carboxylates and *N*-heterocyclic ligands are underway in our lab.

Supplementary material

Crystallographic data reported in this paper have been deposited with the Cambridge Crystallographic Data Center as supplementary publication. CCDC numbers are 878,000 and 878,001. This data can be obtained free of charge via http://www.ccdc.cam.ac.uk/conts/retrieving.html (or from the Cambridge Crystallographic Data Center, 12 Union Road, Cambridge CB2 1EZ, UK; Fax: +44 1223 336 033).

Acknowledgment

We gratefully acknowledge the financial support by the National Natural Science Foundation of China (No. J0830412).

References

[1] L.G. Beauvais, J.R. Long. *Inorg. Chem.*, **45**, 236 (2006).
[2] N.R. Kelly, S. Goetz, S.R. Batten, P.E. Kruger. *CrystEngComm.*, **10**, 68 (2008).
[3] Y.L. Liu, J.F. Eubank, A.J. Cairns, J. Eckert, V.C. Kravtsov, R. Luebke, M. Eddaoudi. *Angew. Chem., Int. Ed.*, **46**, 3278 (2007).
[4] J. Yang, J.F. Ma, Y.Y. Liu, J.C. Ma, S.R. Batten. *Inorg. Chem.*, **46**, 6542 (2007).
[5] H.Y. Liu, H. Wu, J.F. Ma, Y.Y. Liu, B. Liu, J. Yang. *Cryst. Growth Des.*, **10**, 4795 (2010).
[6] Q. Hua, Y. Zhao, G.C. Xu, M.S. Chen, Z. Su, K. Cai, W.Y. Sun. *Cryst. Growth Des.*, **10**, 2553 (2010).
[7] M. Tabatabaee, M.A. Sharif, F. Vakili, S. Saheli. *J. Rare Earths*, **27**, 356 (2009).
[8] Y.J. Mu, J.H. Fu, Y.J. Song, Z. Li, H.W. Hou, Y.T. Fan. *Cryst. Growth Des.*, **11**, 2183 (2011).
[9] S.L. Liu, Y. Yang, Y.F. Qi, X.R. Meng, H.W. Hou. *J. Mol. Struct.*, **975**, 154 (2010).
[10] M.O. Awaleh, A. Badia, F. Brisse. *Cryst. Growth Des.*, **6**, 2674 (2006).
[11] R.P. Feazell, C.E. Carson, K.K. Klausmeyer. *Inorg. Chem.*, **45**, 2635 (2006).
[12] H.K. Chae, D.Y. Siberio, J. Kim, Y. Go, M. Eddaoudi, A.J. Matzger, M. O'Keeffe, O.M. Yaghi. *Nature*, **427**, 523 (2004).
[13] X.L. Wang, Y.Q. Chen, G.C. Liu, H.Y. Lin, J.X. Zhang. *J. Solid State Chem.*, **182**, 2392 (2009).
[14] M. Altaf, H. Stoeckli-Evans. *Polyhedron*, **29**, 701 (2010).
[15] X.R. Meng, X.J. Wu, D.W. Li, H.W. Hou, Y.T. Fan. *Polyhedron*, **29**, 2619 (2010).
[16] C.Y. Niu, B.L. Wu, X.F. Zheng, H.Y. Zhang, H.W. Hou, Y.Y. Niu, Z.J. Li. *Cryst. Growth Des.*, **8**, 1566 (2008).
[17] J.S. Varela, A.J. Mota, H. Aouryaghal, J. Cano, A.R. Diéguez, D. Luneau, E. Colacio. *Inorg. Chem.*, **47**, 8143 (2008).
[18] C. Biswas, P. Mukherjee, M.G.B. Drew, C.J. Gomez-Garcia, J.M. Clemente-Juan, A. Ghosh. *Inorg. Chem.*, **46**, 10771 (2007).
[19] R. Pellicciari, M. Curini, N. Spagnoli, P. Ceccherelli. *Synthesis*, **98**, 629 (1981).
[20] G.M. Sheldrick. *Acta Cryst.*, **A64**, 112 (2008).
[21] X.R. Meng, W. Zhou, Y.F. Qi, H.W. Hou, Y.T. Fan. *J. Organomet. Chem.*, **695**, 766 (2010).

[22] K. Nakamoto. *Infrared and Raman Spectra of Inorganic and Coordination Compounds. Part B*, 6th Edn, p. 64, Wiley, Hoboken, NJ (2009).

[23] X. Shi, G.S. Zhu, X.H. Wang, G.H. Li, Q.R. Fang, G. Wu, G. Tian, M. Xue, X.J. Zhao, R.W. Wang, S.H. Qiu. *Cryst. Growth Des.*, **5**, 207 (2005).

[24] W.J. Chu, X.H. Lou, Z.Y. Wang, C.Y. Xu, Y.T. Fan, H.W. Hou. *J. Coord. Chem.*, **64**, 4373 (2011).

[25] Y. Bai, H. Gao, D.B. Dang, W.L. Shang, X.J. Pan. *J. Mol. Struct.*, **934**, 53 (2009).

[26] R. Wang, L. Han, F.L. Jiang, Y.F. Zhou, D.Q. Yuan, M.C. Hong. *Cryst. Growth Des.*, **5**, 129 (2005).

[27] L.L. Wen, Y.Z. Li, Z.D. Lu, J.G. Lin, C.Y. Duan, Q.J. Meng. *Cryst. Growth Des.*, **6**, 530 (2006).

[28] J. Xia, B. Zhao, H.S. Wang, W. Shi, Y. Ma, H.B. Song, P. Cheng, D.Z. Liao, S.P. Yan. *Inorg. Chem.*, **46**, 3450 (2007).

[29] R.Q. Fan, Y.J. Zhang, Y.B. Yin, Q. Su, Y.L. Yang, W.L.J. Hasi. *Synth. Met.*, **159**, 1106 (2009).

[30] S.Q. Liu, T. Kuroda-Sowa, H. Konaka, Y. Suenaga, M. Maekawa, T. Mizutani, G.L. Ning, M. Munakata. *Inorg. Chem.*, **44**, 1031 (2005).

[31] X.L. Wang, J.X. Zhang, L.L. Hou, G.C. Liu, H.Y. LIN, A.X. Tian. *J. Coord. Chem.*, **64**, 1177 (2011).

[32] S. Caglar, Z. Heren. *J. Coord. Chem.*, **64**, 1289 (2011).

[33] R.H. Cui, G.J. Xu, Z.H. Jiang. *J. Coord. Chem.*, **64**, 222 (2011).

[34] S.Q. Guo, D. Tian, Y.H. Luo, H. Zhang. *J. Coord. Chem.*, **65**, 308 (2012).

[35] L.N. Yang, Y.X. Zhi, J.H. Hei, J. Li, F.X. Zhang, S.Y. Gao. *J. Coord. Chem.*, **64**, 2912 (2011).

[36] T. Li, X. Su, Y. Xiu, X.R. Meng. *J. Coord. Chem.*, **65**, 1792 (2012).